REBUILDING OF ICOTOM RADIOMETER DATA DURING SCHIAPARELLI MARTIAN ENTRY

J. Annaloro[1], P. Boubert[2], A. Bultel[2], M. Jacquot[2], M. Lesage[2], M.C. Druguet[3], D. Vacher[4], S. Ménecier[4], E. Duffour[4], F. Perisse[4], V. Lago[5], N. Rembaut[5], A. Soufiani[6], P. Rivière[6], M. Spel[7], S.T. Surzhikov[8], and D. Yatsukhno[8]

[1]*CNES, Toulouse, France*
[2]*CORIA, Saint-Étienne-du-Rouvray, France*
[3]*IUSTI, Marseille, France*
[4]*Institut Pascal, Clermont-Ferrand, France*
[5]*ICARE, Orléans, France*
[6]*EM2C, Gif-sur-Yvette, France*
[7]*R-Tech, Verniolle, France*
[8]*IPMech, Moscow, Russia*

ABSTRACT

In spite of the crash of Schiaparelli in October 2016, following a nevertheless successful aerothermodynamic entry, data from the infrared radiometers ICOTOM embedded of the COMARS modules was sent to the orbiter before and after the blackout phase. Three pairs of radiometers were located in line on the backshield of the probe in order to monitor the infrared radiation received by the thermal protection system from CO and CO_2 molecules. Teams from different laboratories joined to develop models and experimental analysis in order to extract scinetific knowledge from the recorded data.

Key words: Exomars 2016; Schiaparelli; Martian atmospheric entry; infrared radiation.

1. OBJECTIVES OF THE ICOTOM RADIOMETERS ON SCHIAPARELLI

CNES (Centre National d'Études Spatiales - The French Space Agency) set a consortium of laboratories and companies in order to derive irradiance data from the measurements made by the ICOTOM radiometers during Schaparelli Martian entry within the Exomars 2016 mission and to be able to rebuild the infrared (IR) radiative field around the probe. These radiometers are basically made of a sensor, a filter and a fiber optics as shown on Fig. 1. An important fact is the collection solid angle of the fiber optics that allows to collect radiation in a narrow cone (half angle 17.5) downstream to the probe back shield. The radiometers are embedded on the COMARS modules that are set along a line into the Schiaparelli back cover. Each COMARS module contains two ICOTOM radiometers, so called B1 and B2 in the following, with different filters able to detect radiation in two different midinfrared ranges. B1 spectral range allows to record CO_2 cold bands and CO rovibrational transitions while B2 spectral range corresponds to CO_2 hot bands. More details about the way the COMARS modules are set in the heat shield are given in [1] but Fig. 2, adapted from that article, explained how the six ICOTOM radiometers, with their reference numbers, are located along with the three COMARS modules. The total radiometer installed on the edge of the shield also provided valuable data that can be compared to the ICOTOM radiometer data in the COMARS3 module.

Within this study, the objective of CNES is mainly to improve TPS (Thermal Protection System) design and to limit the margins for the afterbody heat shield by a better IR radiative flux quantification during the descent module Schiaparelli entry. Nevertheless, the objectives of the consortium are more connected to the Schiaprelli mission. They consist in answering to the following questions: What is the meaning of ICOTOM data in terms of radiative flux density? What was the chemical composition of the afterbody plasma? What was the thermodynamic (equilibrium-nonequilibrium) status of the plasma? Which molecular transitions contribute to the IR afterbody radiation? In order to reach those purposes, a global strategy was set including a review of the ICOTOM calibration data necessary to get irradiances from the ICOTOM rough signals, a study of the behaviour of ICOTOM radiometers in front of laboratory plasmas, the development of a state-to-state model for CO_2 kinetics as well as a non-equilibrium radiative model for this molecule, and numerical calculations, including the previous models, in order to rebuild the flowfield around Schiaparelli and the irradiances measured during the entry.

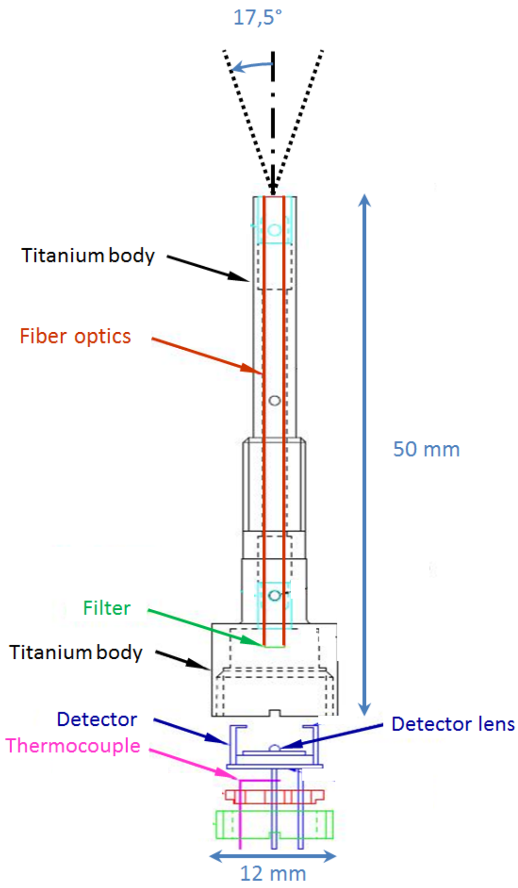

Figure 1. Sketch of an ICOTOM radiometer with especially the semi-angle of collection of the fiber optics.

2. CALIBRATIONS - FLIGHT DATA ANALYSIS

Some calibrations were made by the ICOTOM manufacturer, Le Verre Fluoré (LVF), and by DLR, that was responsible of the COMARS modules. Moreover some complementary calibration data are available for spare models (04QMB1 and 07QMB2) from calibration tests carried out after the flight. The reason of those post-flight tests is the unexpected COMARS temperature during the entry phase (-27^{o}C). Unfortunately, no tests were performed with the flight models at a so low temperature and spare models were used to know the behaviour of the ICOTOM siganl at low temperatures. Indeed, as it can be seen on Fig. 3 and 4, the ICOTOM signals depends on its own temperature, especially for B1. Moreover departures between LVF and DLR calibrations were found. A careful review and complementary tests carried out in CORIA, allowed to conclude that the DLR calibration was more reliable. The DLR data together with the CORIA data has then been used to derive the hemispheric irradiances for the S2 point of Fig.5, about 2 kW.$^{-2}$ for ICOTOM B2 and 5 kW.$^{-2}$ for ICOTOM B1 (besides ICOTOM 08FMB1 around 8 kW.$^{-2}$). Considering that a part of the radiation collected by the ICOTOM B1 is also collected by the ICOTOM B2, a comparison can be made

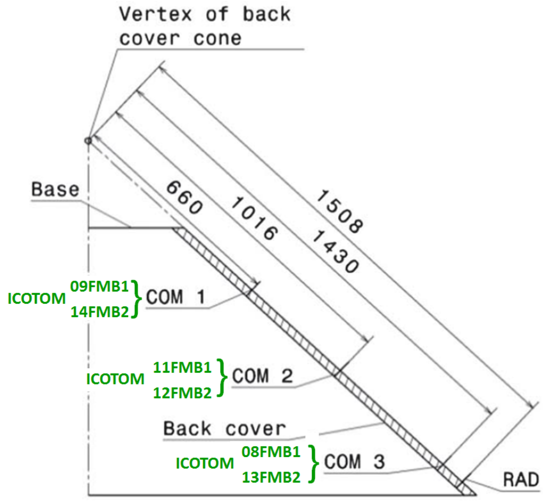

Figure 2. Locations of the ICOTOM radiometers in the COMARS module on the back cover of Schiaparelli.

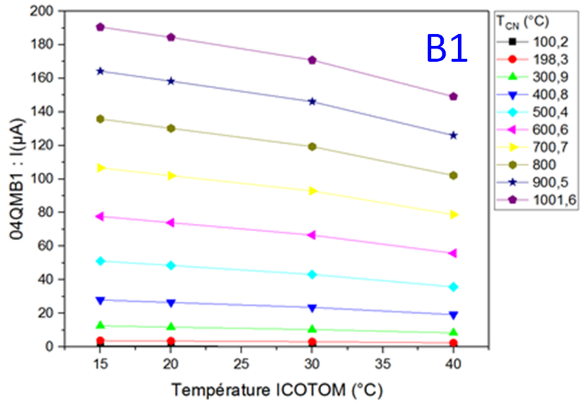

Figure 3. Dependance of the ICOTOM radiometer B1 signal on their own temperature.

between the value obtained by the total radiometer (9 $\pm$ 1,2 kW.m^{-2} [1]) and the corrected values provided by ICOTOM 08FMB1 and 13FMB2 (10,3 $\pm$ 0,9 kW.m^{-2}). The agreement is quite satisfying so far. It is nevertheless necessary to notice the main sources of uncertainty about the ICOTOM temperatures during the netry phase ($\pm$3K) and the relative behaviour between the flight models and the spare model used for calibration.

Results are here given in terms of hemipheric irradiance but, considering that both the total radiometer and the ICOTOM radiometers has an angle of collection and that the plasma is not homogeneous in front of them, further results should be given by unit of solid angle.

3. EXPERIMENTAL STUDIES

In order to better understand, the signal delivered by the ICOTOM radiometers when they are exposed to a non-equilibrium plasmas, some of them was exposed to lab-

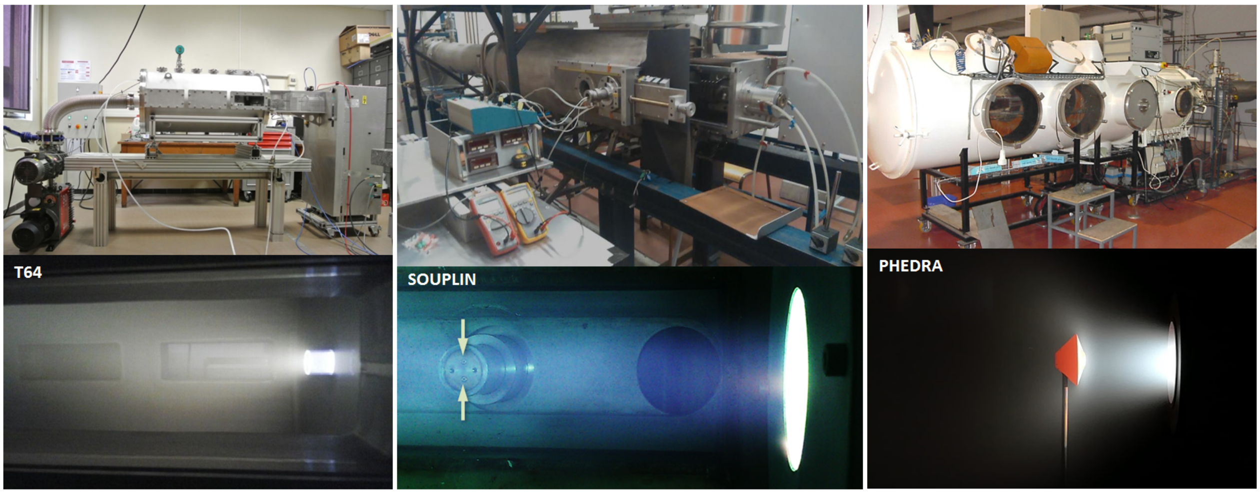

Figure 6. The three plasma wind tunnels used in the experimental part of the study.

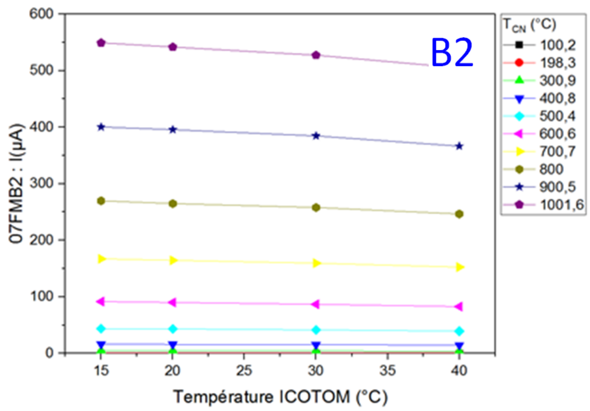

Figure 4. Dependance of the ICOTOM radiometer B1 signal on their own temperature.

oratory plasma jet corresponding to various conditions of enthalpy, pressure and non-equilibrium. The selected wind tunnels are presented on Fig. 6. Those facilities are:

- T64, a subsonic ICP with intermediate enthalpy (low power and flow rate) and low pressure [2].
- SOUPLIN, a subsonic ICP with intermediate enthalpy (intermediate power and flow rate) and intermediate pressure [3]
- PHEDRA, a supersocic arcjet with high enthalpy and low pressure with a model [4].

The purpose was to carry out temperatures, density and radiation measurements in the plasma with the ICOTOM radiometers and other equipments. The produced sets of data could be used for chemical kinetic and radiation code validation. As examples, Fig. 7 shows a spontaneous Raman spectrum for the CO molecule togeter with the best fitting calculation, while Fig. 8 shows a two-photon excitation spectrum of atomic oxygen, also with the best simulation. Both spectra were recorded in the SOUPLIN

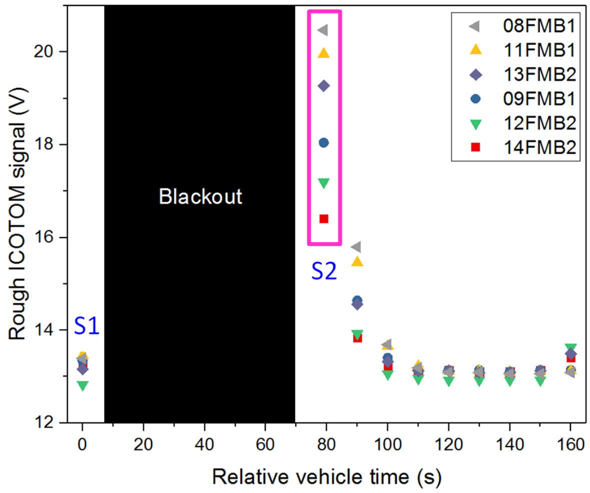

Figure 5. ICOTOM rough flight data.

facility in pure CO_2 plasma. Spontaneous Raman spectroscopy, as well as two-photon laser-induced fluorescence provide microscopic information such as translational, rotational and vibrational temperatures and ground state densities.

4. CHEMICAL KINETICS IN MARTIAN PLASMAS

Concerning chemical kinetics, the challenge was to develop a model for the vibrational structure of CO_2. Such a model had to respect the physical reality (for example Fermi resonances) as well as calculation constraints: being suitable for radiation as well as for chemical calculations, and light enough to be included in aerothermodynamic simulations. A furthe objective was to make the model able to take into account the intermode exchange into CO_2. For the other species, the model CoRaM-

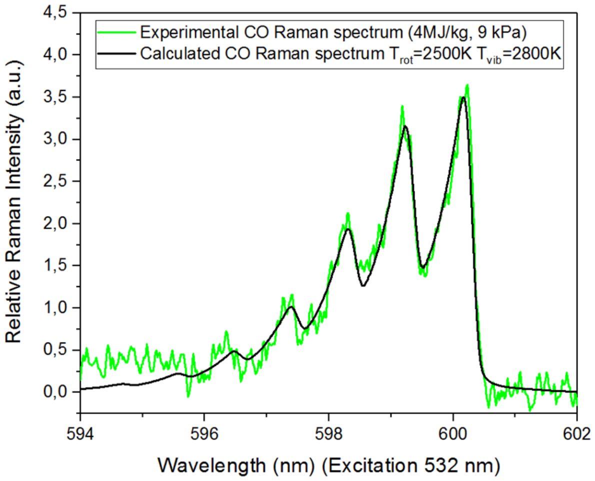

Figure 7. CO pontaneous Raman spectrum in a pure CO_2 plasma together with the best calculated fit.

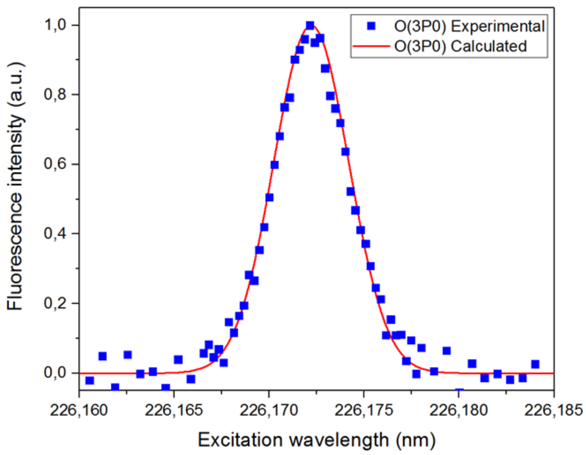

Figure 8. Atomic oxygen Two-photon laser-induced fluorescence excitation spectrum in a pure CO_2 plasma together with the best calculated fit..

Mars [7], developed speciafically for Martian entry studies, was used. In order to calculate, the vibrational energy of CO_2, the equation given by Tashkun et al. [5] and reprocuded in Fig. 9 is used and the results are compared with those of the Hitemp [6] database usually used for infrared radiation calculations at high temperature (Fig. 10). The differences remain reasonable even for relatively high vibrational energies. The following of the work was to make some groups in order to reduce the number of considered levels. This satisfying description of the vibrational structure of CO_2 was implemented in the state-to-state chemical calculations and used for radiative transfer calculation in the plasma surrounding Schiaparelli. However, the production of a reduced model suitable for aerothermodynamic calculations (in order to have a consistent description) is still in progress.

$$
\begin{aligned}
&E(v_1, v_2, l_2, v_3, J=0) = E\left(v_1\, v_2^{\,l_2}\, v_3, J=0\right) \\
&= \sum_i \omega_i \left(v_i + \frac{g_i}{2}\right) + \sum_{i,j} x_{ij}\left(v_i + \frac{g_i}{2}\right)\left(v_j + \frac{g_j}{2}\right) + x_{ll}\, l_2^2 \\
&+ \sum_{i,j,k} y_{ijk}\left(v_i + \frac{g_i}{2}\right)\left(v_j + \frac{g_j}{2}\right)\left(v_k + \frac{g_k}{2}\right) + \sum_i y_{ill}\left(v_i + \frac{g_i}{2}\right) l_2^2 \\
&+ \sum_{i,j,m,n} z_{ijmn}\left(v_i + \frac{g_i}{2}\right)\left(v_j + \frac{g_j}{2}\right)\left(v_m + \frac{g_m}{2}\right)\left(v_n + \frac{g_n}{2}\right) \\
&+ \sum_{i,j} z_{ijll}\left(v_i + \frac{g_i}{2}\right)\left(v_j + \frac{g_j}{2}\right) l_2^2 + z_{llll}\, l_2^4
\end{aligned}
$$

Figure 9. Equation used for the calculation of the CO_2 vibrational energies [5].

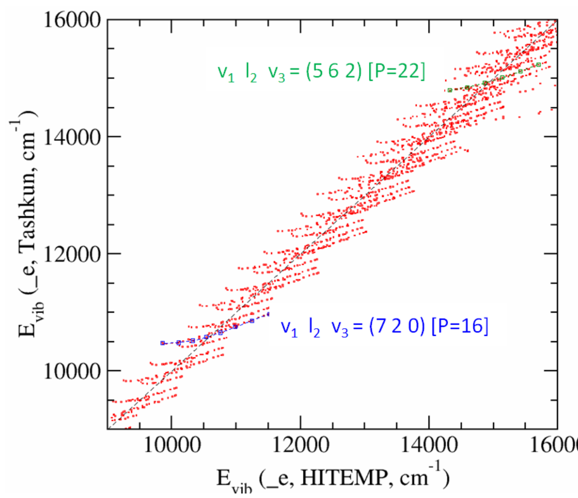

Figure 10. Comparison between Tashkun and HITEMP energy levels.

5. NON EQUILIBRIUM RADIATIVE TRANSFER

The radiative contribution to the flux on Sciaprelli backshield was determine using a ray-tracing method. The radiative transfer equation is solved along each ray by considering the radiative properties of the medium (besides scattering). As vibrational non-equilibrium is expected in the plasma, calculations have to take into account different distribution models from the local thermal equilibrium (1T) to the state-to-state distribution. An intermediate description is to assign a specific temperature to the three vibrational modes of CO_2. Practically, the first and second modes are so coupled that two temperature T_{12} and T_3 are sufficient together with the transletional temperature supposed to be equal to the rotational one. As described previouly, introducing non-equilibrium in the CO_2 vibrational distribution is a challenge but is necessary because of its effects on the infrared radiation on Schiaparelly bachshield [8]. As an example, non-equilibrium conditions encountered in a conical nozzle was used to illustrated the difference with an equilibrium situation (Fig. 11).

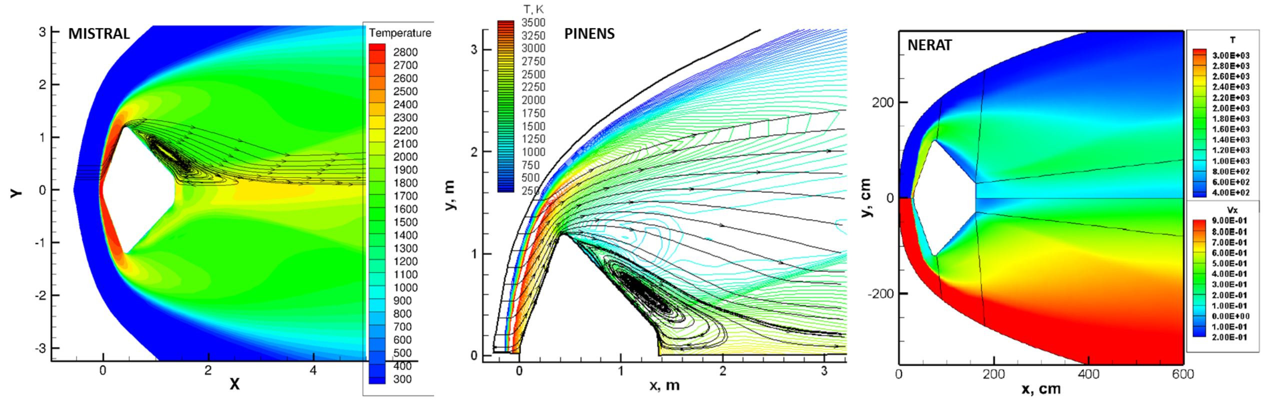

Figure 12. Temperature map in the flowfield around Schiaparelli calculated by the three codes used in the numerical part of the study.

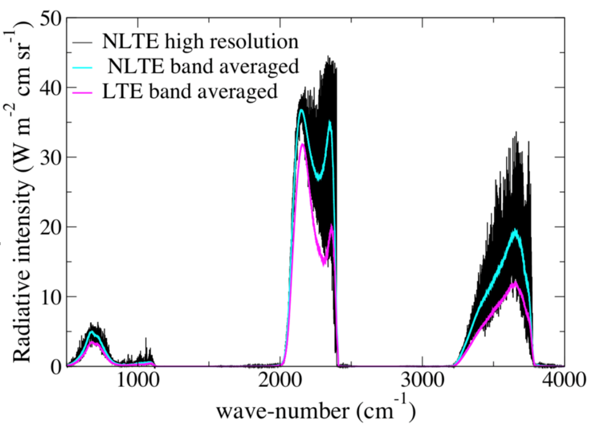

Figure 11. Non-equilibrium spectrum calculated in a conical nozzle expanding jet in 70%N_2, 20%CO_2, 10%H_2O.

6. FLOWFIELD AND HEAT FLUXES

As for facilities, different approaches and codes were used to reproduce the flowfield and the thermodynamic conditions around Schiaparelli:

- MISTRAL is an engineer-oriented code able to integrate advanced models [9].
- PINENS is an academic code able to deal with radiative transfer (ray tracing) and state-to-state model [10].
- NERAT is a global approach code with surface interactions, turbulence, and specific fluxes [11] .

To illustrate, the results of each code, Fig. 12 show the temperature maps calculated around Schiaparelli for a given time. An important issue at the connection between aerothermodynamic and chemical calculations is the dissociation rate of CO_2. Many models were proposed over the past years and a review was made to quantify the influence of that parameter of the flowfield. In relation to that issue, the vibrational relaxation of CO_2 and CO was especially studied to quantify its influence on the flowfield. Evidences of a lower CO_2 recombination appeared close to Schiaparelli surface when vibrational relation is carefully taken into account. First results concerning the radiave fluxes are in good agreement with the ICOTOM measurements especially close to the shield edge where ICOTOM and total radiometer measurements are available. For the other locations, corresponding to the other COMARS modules (see Fig.2), the present calculations performed with NERAT seem to underrestimate the radiative flux. Because, no measurements were recovered from the blackout phasis, it is interresting to try to rebuild the missing entry parameters and the comprehensive trajectory from the past Martian missions. It is shown on Fig.14. By validating the calculations made for the available trajectory points and using the rebuilt trajectory, a satisfying knowledge of the infrared radiative flux on the Schiparelli backshield can be expedted in the next months.

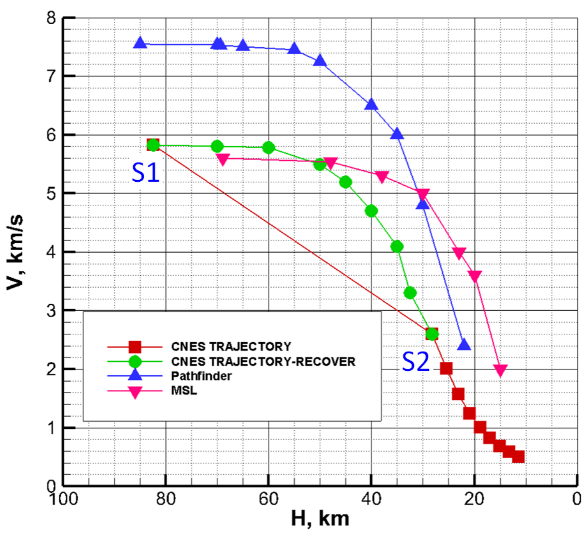

Figure 14. Rebuilding of Schiaparelli trajectory from previous Martian missions.

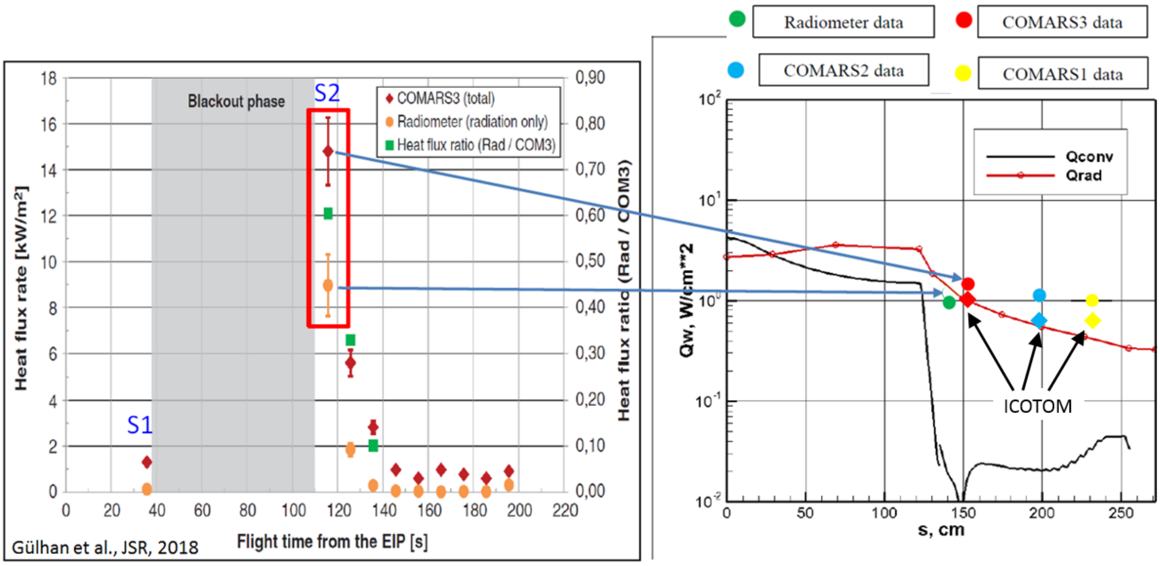

Figure 13. Comparison between radiative and total fluxes measured during Schiaparelli entry and calculated by NERAT.

7. CONCLUSIONS AND OUTLOOKS

Efforts were made to derive absolute flux densities from the ICOTOM measurements. The rebuilding of the flowfield around Schiararelli showed that an accurate description of the CO_2 vibrational structure was of the utmost importance in order to predict the afterbody infrared radiative flux in a non-equilibrium situation. Numerical simulations including state-to-state kinetics and radiative transfer are now in progress to be compared to the ICOTOM meausrements and to be able to predict fluxes for next Martian misions.

ACKNOWLEDGMENTS

The authors would like to thank André Dubus at CNES for the financial support of the activity, Ali Gülhan and the DLR team for the ICOTOM calibration and integration, ESA, TAS-I, DEIMOS for the post-processing of flight data, and Amelia for the attitude reconstruction.

REFERENCES

[1] Gülhan, A. et al. (2018). Aerothermal Measurements from the ExoMars Schiaparelli Capsule Entry. Journal of Spacecraft and Rockets, 56(1), 68-81.

[2] Vacher, D. et al. (2010, July). Diagnostics of an ICP torch by OES and laser interferometry for the study of atmospheric re-entries (Mars, Titan). In 15th Conference on Plasma Physics and Applications (CPPA2010).

[3] Brémare, N., Jouen, S., Boubert, P. (2016). Non-equilibrium radiation during SiC-CO_2 plasma interaction. J. of Physics D: Applied Physics, 49(16), 165201.

[4] Lago, V. (2015). Radiation Measurements in Low Pressure High Enthalpy Flows from VUV to near IR region. In 20^{th} AIAA Int. Space Planes and Hypersonic Systems Technologies Conference (p.3516).

[5] Tashkun, S. A., Perevalov, V. I. (2011). CDSD-4000: High-resolution, high-temperature carbon dioxide spectroscopic databank. J. of Quantitative Spectroscopy and Radiative Transfer, 112(9), 1403-1410.

[6] Rothman, L. S., et al., J. (2010). HITEMP, the high-temperature molecular spectroscopic database. J. of Quantitative Spectroscopy and Radiative Transfer, 111(15), 2139-2150.

[7] Annaloro, J., Bultel, A., Omaly, P. (2014). Elaboration of collisional-radiative models applied to Earth and Mars entry problems. In Journal of Physics: Conference Series (Vol. 550, No. 1, p. 012049). IOP Publishing.

[8] Binauld, Q., Rivière, P., Soufiani, A. (2019). CO_2radiation in expanding flows under vibrational non-equilibrium conditions. In Proceedings of the 9th International Symposium on Radiative Transfer, RAD-19. Begel House Inc..

[9] Vérant, J. L., Spel, M., Bonnal, B. (2010, June). EXOMARS Capsule Aerodynamic Analysis. In 10th AIAA/ASME Joint Thermophysics and Heat Transfer Conference (p. 4646).

[10] Bédon, N., Druguet, M. C., Zeitoun, D., Boubert, P. (2009). Assessment of the convective and radiative transfers to the surface of an orbiter entering a Mars-like atmosphere. In Shock Waves (pp. 541-546). Springer, Berlin, Heidelberg.

[11] Yatsukhno, D., Surzhikov, S., Andrienko, D., Annaloro, J., Omaly, P. (2019). Different Estimations of the Convective and Radiative Heating for the Martian Entry Probes. In AIAA Scitech 2019 Forum (p. 0793).